

Comparison of Electrokinetic Properties of Colloidal Fullerenes (n -C₆₀) Formed Using Two Procedures[†]

JONATHAN BRANT, HÉLÈNE LECOANET, MATT HOTZE, AND MARK WIESNER*

Department of Civil & Environmental Engineering, Rice University, Mail Stop 317, Houston, Texas 77251-1892

In this study we report on the electrokinetic behavior of colloidal aggregates of C₆₀ fullerenes (n -C₆₀) produced through two different techniques: solvent exchange and extended mixing with water. In the first technique, used to produce colloidal materials in several recent toxicity and transport studies, an organic solvent such as tetrahydrofuran (THF) is used to dissolve the C₆₀ before mixing with water. The second technique is more indicative of conditions that might occur in natural aquatic systems. Both types of n -C₆₀ were observed to be negatively charged under a variety of solution chemistries; however, the n -C₆₀ formed using THF was more strongly charged. We conclude that n -C₆₀ likely acquires charge through charge transfer from the organic solvent (when present) and surface hydrolysis reactions. Nevertheless, C₆₀ is capable of acquiring charge and becoming dispersed as n -C₆₀ in water without the aid of organic solvents, a pathway that may be important in determining the mobility of fullerenes in natural systems. These findings also show that n -C₆₀ made using THF retains a portion of the solvent in the cluster structure, subsequently influencing the characteristics of the n -C₆₀ and possibly requiring a re-interpretation of results from recent studies on n -C₆₀ toxicity using THF-derived materials.

Introduction

Beginning with their discovery in 1985 by Kroto et al. (1), fullerenes have received a considerable amount of attention from researchers due to their many unique characteristics (2–6). Particularly, Buckminsterfullerene (C₆₀) has been the focus of numerous investigations (e.g., refs 4, 5, and 7–15) due to its accessibility and potential commercial applications (e.g., electronics materials, superconductors, and sensors). Nevertheless, one of the more intriguing aspects of C₆₀ remains a relative mystery, this being its acquisition of charge and ability to form relatively stable clusters (n -C₆₀) in aqueous systems. Repulsive electrostatic interactions have been cited as the principle mechanism behind the stability of the n -C₆₀ in aqueous solutions despite the strong hydrophobic character and van der Waals properties of the C₆₀ molecules (4, 13, 16). This aspect of C₆₀ is particularly intriguing as it is naturally nonionogenic and may provide a more complete

understanding of how it will behave in natural systems, which becomes increasingly important as these materials are released into the environment. For example, the charge properties of fullerene particles are likely to be important in determining the dynamics of colloidal C₆₀ transport and deposition.

Due to the chemical characteristics of C₆₀ (i.e., uncharged and hydrophobic), a variety of methods have been developed to solubilize and disperse it in solution (4, 6, 10). These techniques commonly require that the C₆₀ first be dissolved in an organic solvent and then dispersed in water through an exchange of solvent and water molecules. This implies that in natural aquatic systems C₆₀ would not be mobile and would instead either settle from solution as a result of aggregation processes or become adsorbed to other hydrophobic surfaces. However, because the charging mechanism(s) for both modified and unmodified C₆₀ is unclear, its behavior in aqueous systems remains speculative given the significance of electrostatic interactions in colloidal phenomena.

Most surfaces in aqueous systems acquire a surface charge through surface dissociation, ion adsorption from solution, or crystal lattice defects (17). Although C₆₀ molecules do not have any ionogenic functional groups (10), previous investigators have measured a negative surface potential in the range of –9 to –30 mV for in pH range of 5–6 (4, 13) for aggregates of C₆₀. To explain this phenomenon a number of theories have been put forth as to the origin of charge for C₆₀, including the adsorption of other ionic species (e.g., hydroxyl ions), charge transfer from the guest solvent (e.g., THF), and protolytic processes stemming from water structuring at the C₆₀ surface (4, 10, 13). However, these theories stem only from observations of n -C₆₀ in simple solutions and may not fully describe the charge behavior of n -C₆₀ in more complex and environmentally relevant solutions. Additionally, each of the proposed theories is ultimately based on the strong electron-acceptor properties of the C₆₀ molecule and thus appears to be central to an understanding of its charge properties regardless of the dispersing media.

C₆₀ molecules are strong electron acceptors (C₆₀ electron affinity = 2.7 eV) (18), allowing them to participate in electron donor–acceptor interactions with water molecules and other potential electron donors (19). In turn, a number of routes exist by which the C₆₀ may become charged depending upon the chemistry of the dispersing medium. In water, a type of hydration shell consisting of 20–24 water molecules may form around the C₆₀ molecule (i.e., hydrophobic structuring) and subsequently undergo hydrolysis reactions with the C₆₀ (10). Because the water molecules are strongly polarized at the C₆₀ surface, this arrangement would result in an overall negative surface charge for the C₆₀ due to an electron density shift (10). However, the magnitude of this charge would purportedly also depend on other considerations such as solution pH, ionic constituents, and the presence of other compounds capable of sharing electrons or oxidizing the C₆₀ surface. Therefore, to fully understand the charge characteristics of C₆₀ and, in the end n -C₆₀, an assessment of these varying factors is required and necessary for understanding the behavior of these materials in environmental systems.

This investigation focuses on characterizing the charge characteristics of n -C₆₀ in environmentally relevant electrolyte solutions. In accomplishing this, we report the ζ -potential of n -C₆₀ as a function of electrolyte type, concentration, and solution pH. Ultimately the goal of this study is to aid in identifying the mechanism(s) by which C₆₀ and n -C₆₀ acquire a surface charge in aqueous systems. The results obtained here also provide a quantitative insight into the interfacial

[†] This paper is part of the Charles O'Melia tribute issue.

* Corresponding author phone: (713)348-5129; fax: (713)348-5203; e-mail: wiesner@rice.edu.

interaction characteristics of $n\text{-C}_{60}$ in natural systems and provide a mechanistic basis by which the transport and deposition characteristics of these fullerenes may be understood.

Experimental Section

$n\text{-C}_{60}$ Preparation. In this investigation, two techniques were used for making $n\text{-C}_{60}$, one utilized the formation of water-soluble guest–host complexes using tetrahydrofuran (THF) (4), and a second, relatively new technique in which $n\text{-C}_{60}$ is prepared through extended mixing of C_{60} in water as first discussed by Cheng et al. (20). The first technique is widely accepted and utilized and furthermore represents the majority of $n\text{-C}_{60}$ preparation techniques where $n\text{-C}_{60}$ is formed through guest–host solvent complexes (4). The purpose of the second technique is to support observations concerning the charge properties of the $n\text{-C}_{60}$ obtained via the more widely used first technique. For clarity $n\text{-C}_{60}$ prepared using THF will be denoted as THF/ $n\text{-C}_{60}$ and that produced through mixing alone as aqu/ $n\text{-C}_{60}$ throughout this paper.

In the first method, $n\text{-C}_{60}$ was prepared following the method outlined by Deguchi et al. (4). Here, powdered C_{60} (MER Corporation, Tucson, AZ) was first dispersed molecularly in THF (Fisher Scientific, Houston, TX) at a concentration of 25 mg/L. The mixture was then purged with nitrogen to remove any dissolved oxygen and stored overnight in the dark while being continuously stirred to allow the solution to become saturated with soluble C_{60} . The C_{60} solution was then filtered through a 0.22- μm nylon filter to remove excess solid material. An equal amount of doubly deionized water (DDW) was then added to the THF/ C_{60} filtrate at a rate of 1 L/min, while being continuously stirred. The THF was subsequently removed from the solution using a rotary evaporator (Buchi Rotovap, Flawil, Switzerland) where the more volatile THF was evaporated off at a temperature of approximately 80 °C. This solution (presumably containing only water, $n\text{-C}_{60}$, and as subsequently revealed, small amounts of THF) was filtered through a 0.22- μm nylon filter and stored in the dark. The resulting THF/ $n\text{-C}_{60}$ had a mean particle diameter of 160 nm as determined from light-scattering measurements.

The aqu/ $n\text{-C}_{60}$ was prepared by creating a supersaturated solution of C_{60} in water (DDW). Here approximately 80 mg of powdered C_{60} was added to 100 mL of DDW. The solution was then stirred using a magnetic stirrer at 500 rpm for a period of several weeks. The final solution had a faint brown/yellow color, a characteristic of $n\text{-C}_{60}$ suspensions, and was filtered through a 0.22- μm filter and stored in the dark. The resulting aqu/ $n\text{-C}_{60}$ had a mean particle diameter of 180 nm.

Surface Charge Characterization. The $n\text{-C}_{60}$ charge properties were characterized using electrophoretic mobility measurements to determine the magnitude and sign of charge while potentiometric and conductometric titrations were used to identify surface functionality. Electrophoretic mobility was measured using a Brookhaven Instruments (Holtville, NY) ZetaPALS system. The ZetaPALS system utilizes phase analysis light scattering (PALS) to measure the electrophoretic mobility of charged particles. The operating principles of PALS allows the instrument to analyze particles with a low electrophoretic mobility (down to $10^{-11} \text{ m}^2/\text{Vs}$) and is capable of characterizing particles in the size range of 5–30 000 nm. Solution pH was varied from approximately 1 to 12 and was adjusted by adding appropriate amounts of either 0.05 N NaOH or 0.05 N HCl. When studying the impact of ionic strength on electrophoretic mobility, solution pH was adjusted to pH = 7. All measurements were carried out at 25 °C, which was maintained internally by the ZetaPALS instrument. ζ -potential was calculated from the measured electrophoretic mobility using the Smoluchowski equation

TABLE 1. Selected Physical and Chemical Properties of the Ionic Species Used in This Investigation (23)

ion	bare radius (nm)	hydrated radius (nm)	H_{hyd} (kJ/mol)
Na^+	0.095	0.36	−406
K^+	0.133	0.33	−322
Cl^-	0.181	0.33	−363
OH^-	0.176	0.30	−400
SO_4^{2-}	0.149	0.40	−126
Ba^{2+}	0.135	0.40	−1304
Ca^{2+}	0.099	0.41	−1577
Mg^{2+}	0.065	0.43	−1921

(21). No corrections for polarization and relaxation effects of the electric double layer were required as the ratio of particle diameter to Debye length was ≥ 100 in each case (22).

Electrophoretic mobility was measured using a variety of environmentally relevant mono- and bivalent salts (NaCl , KCl , Na_2SO_4 , CaCl_2 , BaCl_2 , and MgCl_2) (ACS Grade, Fisher Scientific, Pittsburgh, PA) as background electrolytes. Selected properties of the electrolytes used in this investigation are reported in Table 1. The selected ions represent a range of sizes and valences in order to study the impacts of these properties on $n\text{-C}_{60}$ surface charge. The enthalpy of hydration (H_{hyd}) is the amount of energy released when a mole of the ion dissolves in a large amount of water and forms an infinitely dilute solution in the process (23). The H_{hyd} term thus quantifies the state of hydration (i.e., bond strength between the ion and water molecules) for the ionic species. The electrolytes chosen for study were selected for their specific characteristics and their prevalence in aquatic systems.

Potentiometric and conductometric titrations were used to identify the functionality and charge on the $n\text{-C}_{60}$ (24). Potentiometric titrations were carried out using a Hach Company (Loveland, CO) digital titrator having an accuracy of ± 0.01 mL. Solution pH was measured using an Orion Research, Inc. (Boston, MA) digital pH meter, which was calibrated prior to each titration. Solution pH was first adjusted using 12 N HCl to produce an initial pH of approximately 2.4. Solution ionic strength was varied using sodium chloride as a background electrolyte. Prior to each titration the solution was sparged with nitrogen gas (N_2) for 15 min to remove any dissolved oxygen from the solution. The solution was subsequently kept in a nitrogen atmosphere. Conductometric titrations were performed using a Jenco model 1671 (Jenco Electronics, Ltd., Grand Prairie, TX) conductivity meter. All titrations were carried out at a temperature of 25 °C with an $n\text{-C}_{60}$ concentration of 100 mg/L.

Results and Discussion

From Figure 1, the THF/ $n\text{-C}_{60}$ is significantly charged in each of the monovalent electrolyte solutions studied, with the absolute magnitude of the ζ -potential decreasing with increasing ionic strength for each case, in accordance with classical electrostatic theory (21, 23). Similarly, for each of the monovalent electrolytes, the ζ -potential decreased marginally for $10^{-5} < I < 10^{-4}$ M and more substantially at $I > 10^{-3}$ M. Aggregation of the THF/ $n\text{-C}_{60}$ into visibly larger clusters was observed for $I > 10^{-2}$ M for each of the monovalent salts. Separate measurements found that the mean particle size increased to approximately 1 μm after several minutes of mixing in the presence of sodium chloride, confirming that the $n\text{-C}_{60}$ were aggregating in the presence of these salts. Also, a slightly stronger charge was measured for the THF/ $n\text{-C}_{60}$ in the presence of sodium chloride as compared to that measured in the potassium chloride and sodium sulfate solutions, respectively. This indicates that

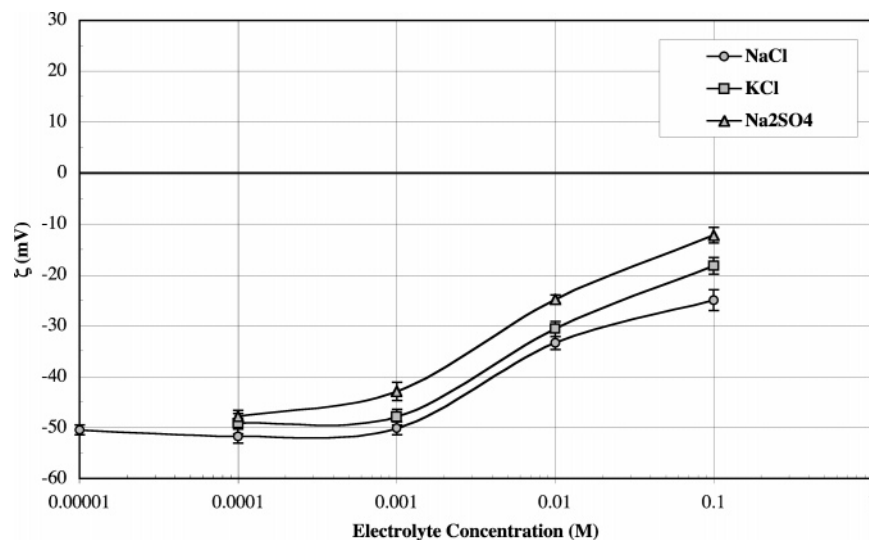


FIGURE 1. ζ -potential measured as a function of monovalent electrolyte concentration on a semilogarithmic scale for the THF/*n*-C₆₀ (pH = 7, *T* = 25 °C, *n* = 10). Error bars represent the standard error of the measurement.

the potassium cation can more effectively screen the THF/*n*-C₆₀ surface charge than the sodium cation. This is attributed to the smaller hydrated radius for the potassium cation, allowing it to more closely approach the charged surface (23). The increased charge neutralization observed for the sodium sulfate results from the fact that each mole of this electrolyte contributes two moles of sodium cations as compared to just one for the sodium and potassium chloride salts. Of note, a negative maximum, in terms of the absolute magnitude of the ζ -potential (as would be indicated by a negative dip in the curve), was not measured for the THF/*n*-C₆₀ in the presence of the sulfate anion (SO₄²⁻) over the ionic strengths studied. This indicates that adsorption of these bivalent coions did not occur and was not contributing to the THF/*n*-C₆₀ surface charge under the conditions studied here (25).

Preferential adsorption of coions (e.g., Cl⁻ and SO₄²⁻) to hydrophobic surfaces has previously been suggested as a charging mechanism for otherwise uncharged or weakly charged hydrophobic surfaces (25). Because anions are less hydrated than cations, as indicated by their lower *H*_{hyd} (Table 1), they can more closely approach a surface. Accordingly, the mechanism by which the negatively charged coions approach a surface and impart a charge is a nonspecific process, meaning that it does not involve a chemical bond to surface groups. Instead, it is only the valence of the coions that determines the magnitude of the charge. However, no absolute maximum was observed for any of the monovalent electrolytes (Figure 1), particularly the sodium sulfate, indicating that coion adsorption was not significant and was not the source of the measured THF/*n*-C₆₀ surface charge (25).

Compared to the monovalent salts, the bivalent electrolytes have an increased screening effect on the THF/*n*-C₆₀ surface charge (Figure 2a) (23); thus ζ -potential decreases more substantially with increasing bivalent cationic strength. For the bivalent cations the THF/*n*-C₆₀ ζ -potential is moderately charged (-30 to -40 mV) at the lower ionic strengths (*I* ≤ 10⁻⁵ M); as ionic strength approaches 10⁻¹ M, the absolute magnitude of the THF/*n*-C₆₀ ζ -potential is reduced to approximately -10 mV. Generally, the magnesium cation was more effective at screening the THF/*n*-C₆₀ surface charge, followed by the barium and calcium cations, respectively. Notably, the calcium cation produced a charge reversal at *I* = 10⁻⁴ M CaCl₂ (ζ = +20 mV), while no such reversal was measured for either the magnesium or barium electrolytes (Figure 2a). A local charge minimum and

maximum were observed for barium at *I* = 10⁻⁴ and 4 × 10⁻⁴ M BaCl₂, respectively. The charge reversal and minima observed for the calcium and barium cations, respectively, suggest that these cations are complexing with the THF/*n*-C₆₀ surface.

Because the THF/*n*-C₆₀ is negatively charged, surface complexation with bivalent cations is electrostatically favorable (26). In complexation reactions an ion may form an inner-sphere complex (chemical bond), an outer-sphere complex (ion pair), or reside in the diffuse electrical double layer (27). Regardless of the type of complex formed, each reduces the absolute value of the surface charge, although to different degrees. The ability of the cations to approach the charged interface is related to their state of hydration (*H*_{hyd}) (Table 1), where smaller ions are more strongly hydrated than larger ones having the same valence (23). Therefore, magnesium is the most strongly hydrated cation followed by calcium and barium, respectively, and is thus less likely to shed any of its bound waters. The inability to shed these waters prevents the magnesium cation from closely approaching the particle, thus resulting in a reduced charge screening capacity. Therefore, the barium and calcium cations respectively, were able to more easily complex with the THF/*n*-C₆₀ surface than the magnesium cation as they could more closely approach the THF/*n*-C₆₀ surface. However, the calcium cation produced a charge reversal while only a minima was observed for the barium, pointing to something beyond just a relationship between charge screening and ion hydration.

Charge reversal occurs when an excess amount of counterions surround a charged surface such that the overall surface charge has a sign opposite that of its actual "bare" charge (17, 21). Although charge reversal is not supported by the Poisson-Boltzmann equation, where counterions can only partially neutralize surface charge, it is a widely accepted phenomenon (17, 21, 23, 28). According to Ravindran and Wu (28) charge reversal does not necessarily result from the specific binding of ions to surface groups but can instead result from an interplay between correlation and excluded volume effects of the counterions. Because the charge reversal measured for the calcium chloride is reversible, it became negative again as ionic strength increased beyond *I* = 10⁻⁴ M CaCl₂, the mechanism of adsorption is electrostatic and not chemical in nature. Thus the behavior of the THF/*n*-C₆₀ ζ -potential as a function of calcium chloride concentration may be described as a balance between co-ion and counterion interfacial concentrations. As ionic strength increases, the

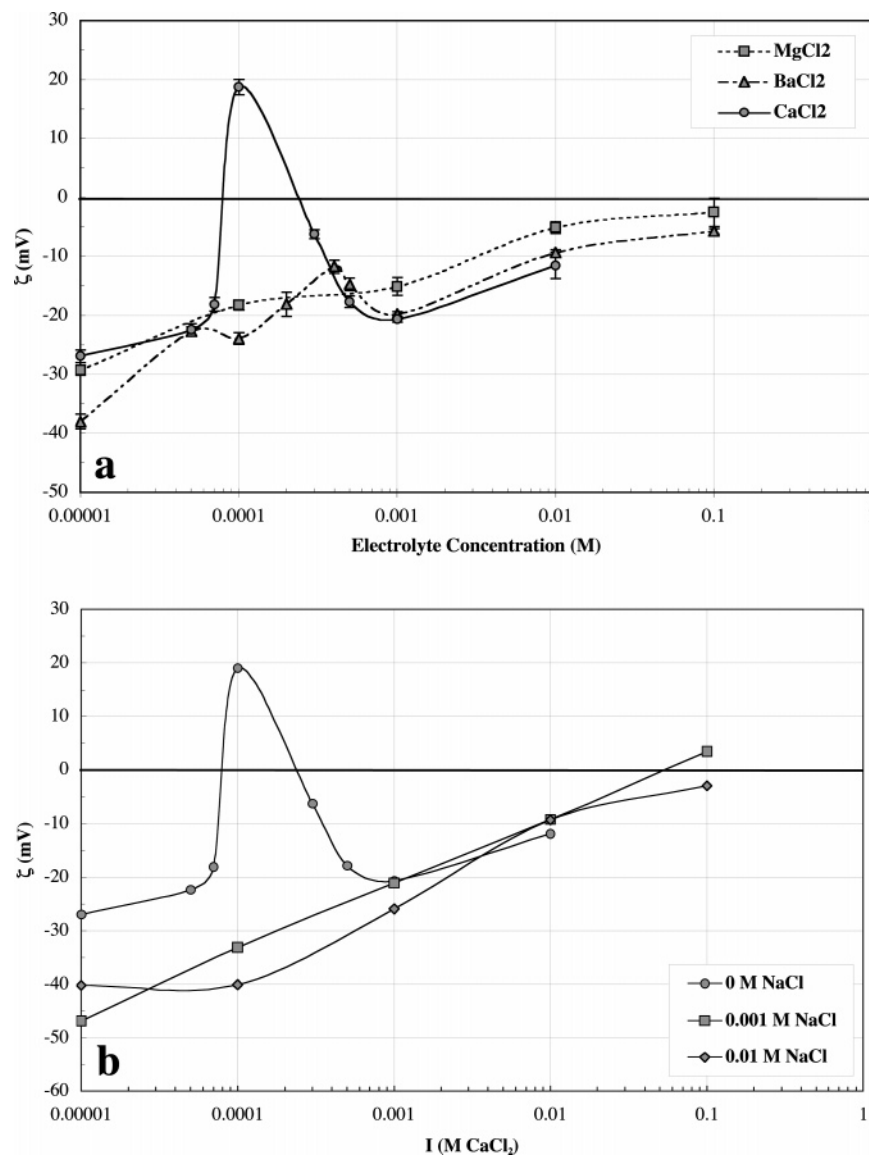


FIGURE 2. (a) ζ -potential as a function of bivalent electrolyte concentration plotted on a semilogarithmic scale for the THF/*n*-C₆₀ (pH = 7, $T = 25^\circ\text{C}$, $n = 10$). Error bars represent the standard error of the measurement. (b) Relationship between THF/*n*-C₆₀ ζ -potential with a background electrolyte concentration of 10^{-4} M CaCl₂ as a function of sodium chloride concentration.

calcium counterions neutralize the THF/*n*-C₆₀ surface charge, eventually resulting in the observed reversal measured at $I = 10^{-4}$ M CaCl₂, at which point the calcium cations overwhelm the bare THF/*n*-C₆₀ surface charge. As the calcium chloride concentration increases beyond $I = 10^{-4}$ M CaCl₂ the concentration of coions (Cl⁻) increases in the THF/*n*-C₆₀ interfacial region, producing an increasingly negative ζ -potential and in turn re-reversing the charge. A similar trend was observed by Elimelech and O'Melia (25) when characterizing the electrostatic properties of hydrophobic latex particles. The proposed mechanism is further supported by measuring THF/*n*-C₆₀ ζ -potential as a function of calcium chloride concentration in the presence of an indifferent electrolyte (i.e., NaCl) (Figure 2b). Here, the addition of sodium chloride and the subsequent increase in the concentration of coions (Cl⁻) in solution prevent or mask the charge reversal observed in the presence of calcium chloride alone. Furthermore, the THF/*n*-C₆₀ is more negatively charged at higher co-ion concentrations (i.e., higher sodium chloride concentrations). Therefore, although the calcium cation was capable of closely approaching the THF/*n*-C₆₀ surface, it is likely that it did not chemically sorb to it. On the other hand, the barium cation was unable to approach

as closely to the charged surface resulting as evidenced by the charge minima and absence of net charge reversal.

***n*-C₆₀ Charge as a Function of pH.** Additional experiments were carried out to characterize THF/*n*-C₆₀ ζ -potential as a function of pH using sodium chloride as a background electrolyte (Figure 3a). Here the absolute value of the ζ -potential increased from approximately -10 mV at around pH = 2 to between -30 to -70 mV at pH = 10, depending on the background ionic strength. The absolute magnitude of the ζ -potential decreased with increasing ionic strength, with the difference becoming more pronounced as the pH became more basic. From Figure 3a, the THF/*n*-C₆₀ was found to have a pH_{iep} around pH = 1.3. This is considerably lower than the reported pH_{iep} for graphite ($\text{pH}_{\text{iep}} \approx 4.5-5.5$), where graphite is positively charged at pH < 5 and negatively charged at pH > 5 (29). The lack of positive and negative branches in the ζ -potential curves in Figure 3a demonstrates that the THF/*n*-C₆₀ surface contains only acidic groups (17). Such surfaces are characterized by a decreasing charge that only reaches zero at sufficiently low (acidic) pH values and an increasingly negative surface charge with increasing pH, as was indeed observed here (Figure 3a) (17).

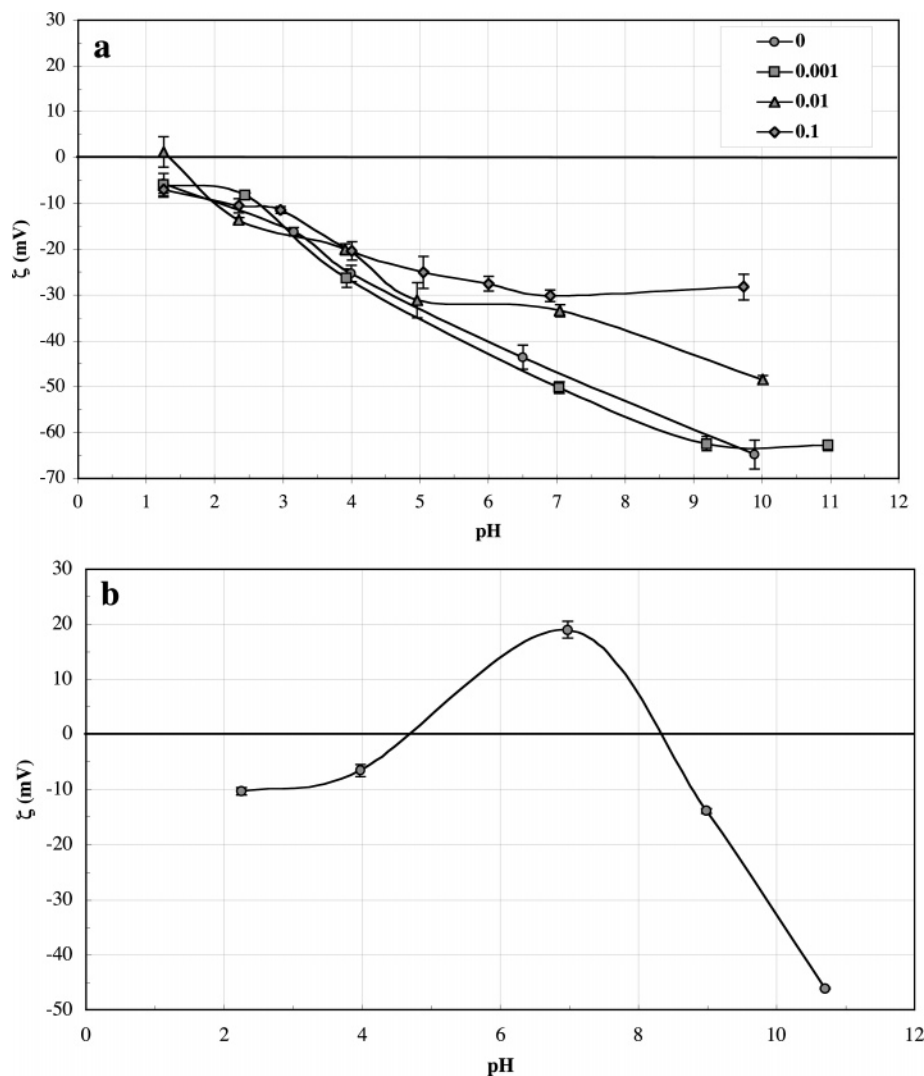


FIGURE 3. (a) THF/*n*-C₆₀ ζ -potential as a function of pH using sodium chloride as a background electrolyte (pH = 7, $T = 25^\circ\text{C}$, $n = 10$). (b) THF/*n*-C₆₀ ζ -potential as a function of pH with an electrolyte concentration of 10^{-4} M CaCl₂ (pH = 7, $T = 25^\circ\text{C}$, $n = 10$). Error bars represent the standard error of the measurement.

Electrophoretic mobility measurements as a function of pH were also conducted using calcium chloride as a background electrolyte to examine the impact of pH on the observed charge reversal at $I = 10^{-4}$ M CaCl₂ (Figure 3b). Under acidic conditions at $I = 10^{-4}$ M CaCl₂, the THF/*n*-C₆₀ is weakly negatively charged. As pH increases, the THF/*n*-C₆₀ acquires a net positive ζ -potential in the neutral pH range, before becoming increasingly negatively charged at pH ≥ 8 . Thus, for pH values that are characteristic of natural aquatic systems (pH = 5–8) *n*-C₆₀ would be positively charged under the reported low hardness conditions ($I = 10^{-4}$ M CaCl₂) and when adsorbing compounds such as natural organic matter do not play a role. Furthermore, based on the data shown in Figure 3b, isoelectric points (pH_{iep}) exist for the THF/*n*-C₆₀ at pH values of approximately 5 and 8 under the given conditions. Therefore, the potential for rapid aggregation of THF/*n*-C₆₀ at these conditions is likely. The observed charge versus pH relationship dramatically differs from that seen for the indifferent sodium chloride as the background electrolyte (Figure 3a) and thus illustrates the significance of electrolyte type on the THF/*n*-C₆₀ charge characteristics (30).

To further characterize the functionality of the THF/*n*-C₆₀ surface a series of conductometric and potentiometric titrations were carried out, which have been extensively shown to be a valuable tool in characterizing the functionality of charged surfaces (17, 27, 31, 32). The conductometric and

potentiometric titration results for THF/*n*-C₆₀ are reported in Figure 4, panels a and b, respectively. The conductometric titration was performed in the absence of any electrolyte while the ionic strength was varied in the potentiometric titrations using sodium chloride. From Figure 4a, the THF/*n*-C₆₀ surface groups are fully dissociated at a base concentration of approximately 4.8×10^{-3} M NaOH, corresponding to a pH of approximately 3.8. At this point there is an inflection in the conductivity curve and the slope becomes positive. The shape of the conductometric curve supports earlier observations made from the ζ -potential as a function of pH data where the THF/*n*-C₆₀ surface was characterized by strong acidic groups (25, 31). For the conductometric curve the ratio of the linear descending and ascending slopes is equal to 1.6, which is greater than the theoretical value of 1.213 for the titration of a strong acid with a strong base at 25°C (31). Furthermore, the relatively sharp inflection point indicates that equilibrium is quickly attained for dissociation of the surface groups, again indicative of strongly acidic groups. This observation is further supported by the shape of the potentiometric titration curves shown in Figure 4b (25). The steep slope of the potentiometric titration curves for the THF/*n*-C₆₀ indicates the presence of strong acid groups, which quickly dissociate with increasing pH. The corresponding $\text{p}K_a$ for the THF/*n*-C₆₀ is equal to approximately 4, in agreement with the conductometric titration results.

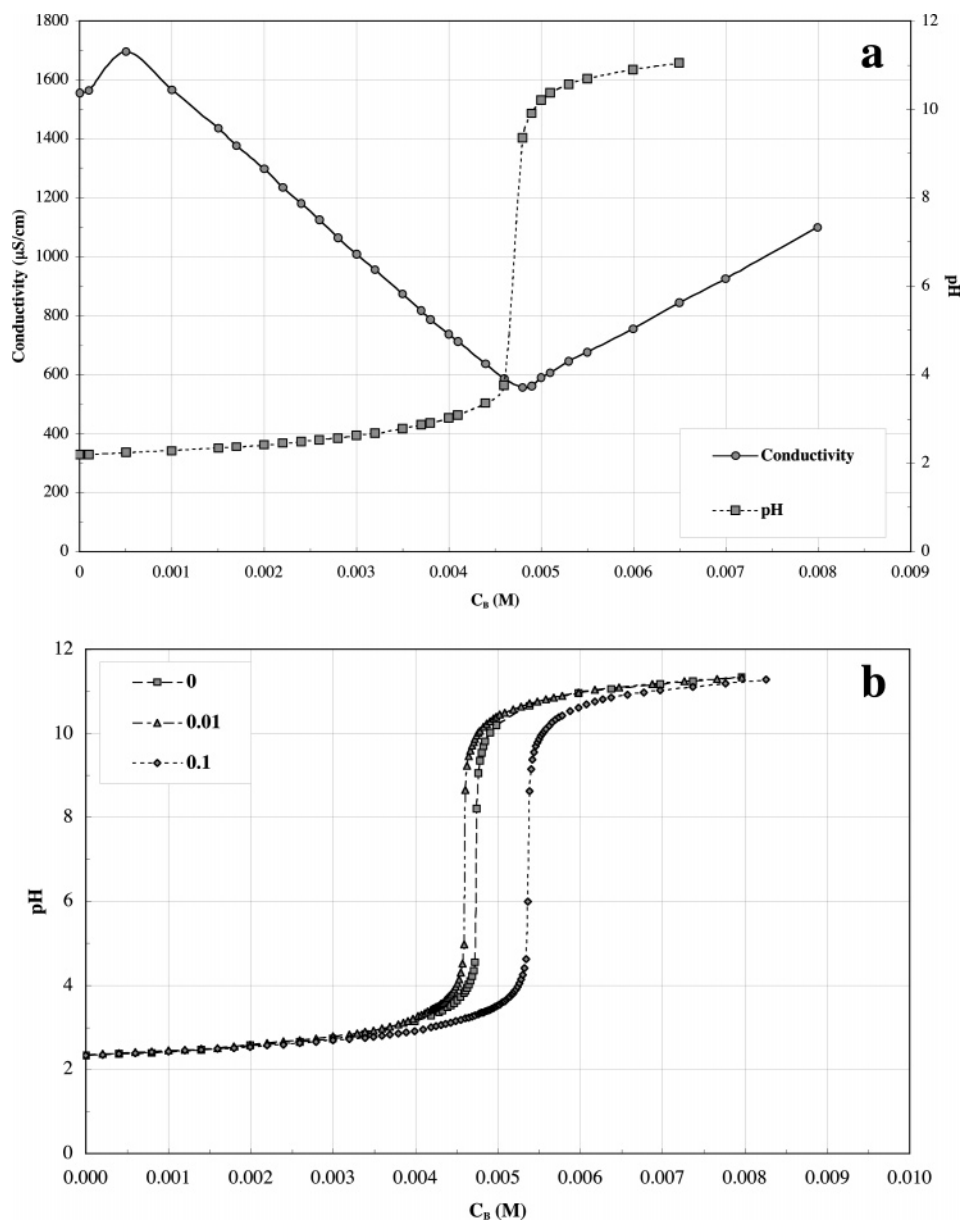


FIGURE 4. Representative (a) conductometric and (b) potentiometric titration curves for THF/*n*-C₆₀ as a function of base (NaOH) concentration (C_b) in doubly deionized water and in electrolyte (NaCl) solutions ($T = 25\text{ }^\circ\text{C}$, $[\text{THF}/n\text{-C}_{60}] = 100\text{ mg/L}$).

Discussion

Based on the results presented thus far, the THF/*n*-C₆₀ is charged in aqueous media and tends to follow expectations based on classical electrostatic theory with aggregation occurring as ionic strength increases or decreasing pH. Furthermore, the strong dependence of THF/*n*-C₆₀ ζ -potential on pH and titration analyses suggest that the THF/*n*-C₆₀ surface is primarily characterized by relatively strong acid groups, which dissociate with increasing pH (17). However, as previously noted, the C₆₀ used here to make the THF/*n*-C₆₀ is not chemically modified and therefore should not initially have any surface functional groups, which would otherwise account for the observed trends. This in turn suggests that the THF/*n*-C₆₀ surface is acquiring ionogenic groups or charge during cluster formation. As noted in the Introduction, a number of theories have been put forth to explain this charge acquisition by similarly prepared *n*-C₆₀ (4, 10, 13). Again, for the THF/*n*-C₆₀ used here, several possibilities exist: co-ion adsorption, charge transfer, co-ordination of water at the *n*-C₆₀ surface, and hydrolysis reactions.

The concept and possibility of co-ion adsorption was touched upon earlier in this manuscript when detailing the charge characteristics of THF/*n*-C₆₀ under various electrolyte chemistries. Adsorption of co-ions by the C₆₀ is likely only for absorption of hydroxyl groups from solution. This is due to the fact that a significant ζ -potential was measured for the THF/*n*-C₆₀ as a function of pH in the absence of any added electrolyte, which would have contributed chloride ions to the solutions (Figure 3a). Furthermore, no increase in the magnitude of the THF/*n*-C₆₀ surface charge was measured in the presence of the sulfate (SO₄²⁻) ion (Figure 1). To further explore co-ion adsorption as a charging mechanism, it is useful to evaluate the charge properties of the *n*-C₆₀ prepared through mixing with water only (aqu/*n*-C₆₀).

To determine the extent to which, or if, hydroxyl ion adsorption contributes to the *n*-C₆₀ surface charge, the pH of the dispersing water was measured just prior to and at various intervals during the mixing process. Over this time no significant change (~1%) in pH was recorded, indicating that the hydroxyl ion concentration did not change considerably even as the aqu/*n*-C₆₀ was being formed. A similar

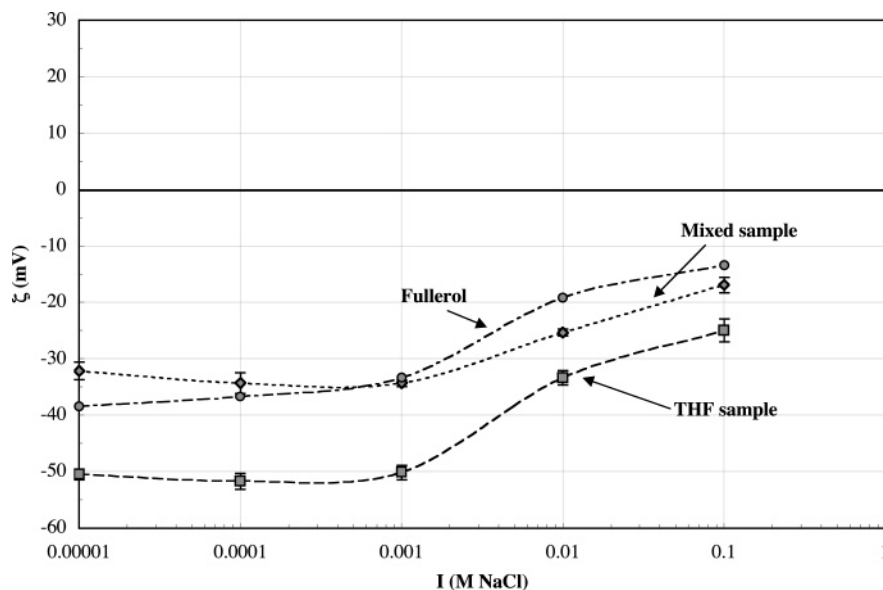


FIGURE 5. Comparison of ζ -potential as a function of electrolyte (NaCl) concentration for THF/*n*-C₆₀, aqu/*n*-C₆₀, and fullerol (pH = 7, T = 25 °C, n = 10). Error bars represent the standard error of the measurement.

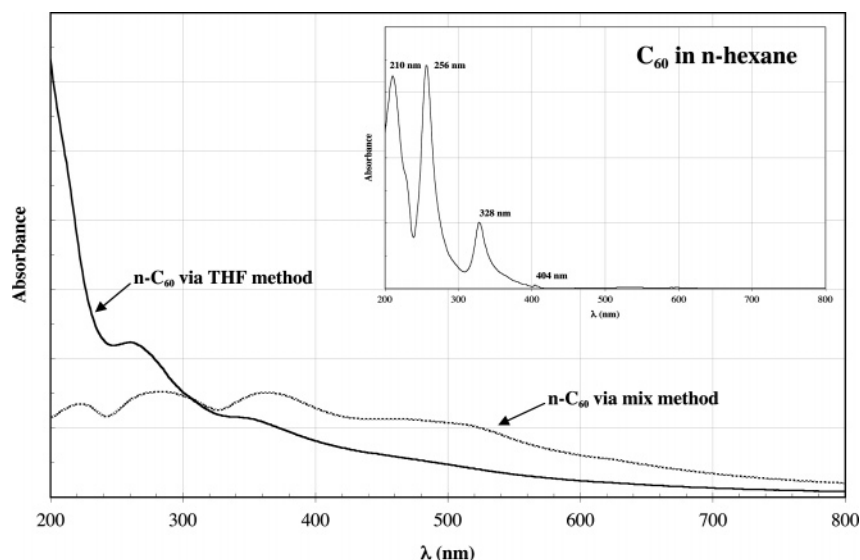


FIGURE 6. UV absorbance spectra of the THF/*n*-C₆₀ and aqu/*n*-C₆₀ in water. The inset shows the UV absorbance spectra of C₆₀ dissolved in *n*-hexane and is considered that of a true solution of C₆₀.

observation was made for the THF/*n*-C₆₀ samples where pH remained relatively unchanged after cluster formation. An additional aqu/C₆₀ sample was prepared having an initial pH of 10.4. For the basic solution the rate of *n*-C₆₀ formation, identified by the change in solution color, was similar to that observed for the aqu/*n*-C₆₀ made at pH = 5.6. Furthermore, the sample prepared at pH = 10.4 was similarly charged as the aqu/*n*-C₆₀ prepared at the lower pH. If adsorption of hydroxyl ions were occurring, it should have resulted in a change (lowering) of pH or potentially in an increased charge for the sample prepared at the higher pH. As neither occurred, it suggests that the C₆₀ molecules do not acquire charge through adsorption of hydroxyl ions alone or are at least capable of acquiring charge through some other mechanism, such as charge transfer and hydrolysis reactions.

Considering that THF/*n*-C₆₀ is formed by first dissolving C₆₀ in THF, it is possible that the THF/*n*-C₆₀ surface charge results from charge transfer between the C₆₀ molecule and THF compound. Charge transfer could occur between the ether oxygen (electron donor) of the THF compound and a C₆₀ molecule (electron acceptor) (4, 10). ζ -potential curves

for the THF/*n*-C₆₀ and aqu/*n*-C₆₀ as a function of ionic strength are similar in shape but differ in their relative values (by approximately 10–20 mV), with the aqu/*n*-C₆₀ having a weaker charge than the THF/*n*-C₆₀ (Figure 5). The measured charge for the aqu/*n*-C₆₀ closely follows that measured for hydroxylated C₆₀ (fullerol), supporting the hypothesis that C₆₀ acquires charge through hydroxylation of its surface either through adsorption of hydroxyl groups or hydrolysis (10). The higher charge measured for the THF/*n*-C₆₀ suggests that charge transfer, and or residual THF, is indeed responsible for some of the overall THF/*n*-C₆₀ surface charge. Residual THF was found by Andrievsky et al. (10) in similarly prepared *n*-C₆₀ using UV absorbance and FTIR analysis, resulting in the observed clathrate crystal like structure of *n*-C₆₀ prepared in this way (4).

Indeed, a dramatic difference existed in the UV absorbance spectra for the THF/*n*-C₆₀ and aqu/*n*-C₆₀ samples (Figure 6). For reference, the absorbance spectra of C₆₀ in *n*-hexane, considered to be that of a true C₆₀ solution (4, 10), is reported in the Figure 6 inset. FTIR analysis of the THF/*n*-C₆₀ used in this investigation also showed characteristic absorption peaks

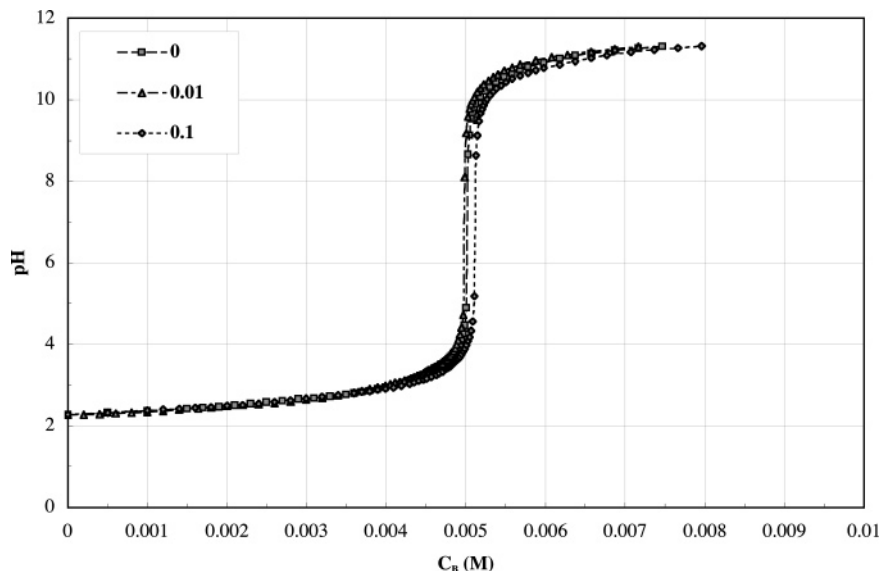


FIGURE 7. Representative potentiometric titration curves for aqu/*n*-C₆₀ as a function of base (NaOH) concentration (*C_B*) in doubly deionized water and in electrolyte (NaCl) solutions (*T* = 25 °C, [aqu/*n*-C₆₀] = 100 mg/L).

for THF, indicating that it was present in the *n*-C₆₀ complex. Compared to the THF/*n*-C₆₀, the absorbance spectra for the aqu/*n*-C₆₀ shifted to the longer wavelength (red shift) and were broader. The THF/*n*-C₆₀ and aqu/*n*-C₆₀ were characterized by absorption peaks at 200, 260, and 349 nm and at 223, 286, and 361 nm, respectively. Absorbance peaks between approximately 330 and 350 nm are characteristic for solvated C₆₀. Both the THF/*n*-C₆₀ and the aqu/*n*-C₆₀ are likely surrounded by ordered layers of water molecules and are hydrated to some extent (10). The extent of hydration is indicated by how significant the changes in the absorption spectra are compared to that for the C₆₀ in *n*-hexane. The broad absorption band between 430 and 530 nm suggests that the aqu/*n*-C₆₀ is more strongly hydrated than the THF/*n*-C₆₀ (10). This broad absorbance band results from the formation of weak donor–acceptor complexes of C₆₀ (electron acceptor) and water (electron donor). The broadening of the spectra bands as compared to the C₆₀ in *n*-hexane is typical of colloidal solutions of fullerenes (C₆₀ aggregates) as a result of their strong light-scattering effects (10). The clear differences in the spectra for the two samples further indicates that THF is present in some form in the *n*-C₆₀ cluster as found by Andrievesky et al. (10) and that it subsequently impacts the magnitude of the *n*-C₆₀ surface charge. Again, this may occur either through the THF being present as a residual compound not specifically interacting with the C₆₀ or through charge transfer between the ether oxygen from the THF compound and the C₆₀ molecule (4) or a combination of both. The presence of residual THF in the *n*-C₆₀ calls into question the interpretation of results from a recent study (33) that concluded that *n*-C₆₀ was highly toxic to cell cultures.

The differences between the THF/*n*-C₆₀ and aqu/*n*-C₆₀ are further demonstrated by comparing the potentiometric titration curves for the two samples (Figures 4b and 7, respectively). In both instances, the steep slope of the titration curves indicates the presence of strong acid groups that easily dissociate from the surface, each with p*K_a* values of approximately pH = 4. However, as compared to the THF/*n*-C₆₀ (Figure 4b), the curves for the aqu/*n*-C₆₀ do not change position as ionic strength increases, indicative of strong acid groups (25). Furthermore, the THF/*n*-C₆₀ became fully dissociated at a lower base concentration than the aqu/*n*-C₆₀. This demonstrates that the aqu/*n*-C₆₀ has a slightly different yet similar surface chemistry as compared to the THF/*n*-C₆₀. This difference can be attributed to the charge transfer and presence of residual THF in the THF/*n*-C₆₀ cluster

structure and the fact that the aqu/*n*-C₆₀ is more strongly hydrated than the THF/*n*-C₆₀.

To explain the observed charge behavior for the aqu/*n*-C₆₀, and ultimately the THF/*n*-C₆₀ as well, the interaction between C₆₀ and water must be considered. Structuring of water molecules at hydrophobic interfaces has previously been identified for graphite (34) and carbon nanotubes (16). In each case, a water layer approximately one water layer thick was measured. However, water structuring does not account for the observed charge properties of *n*-C₆₀. When water molecules structure themselves at hydrophobic interfaces, they do so in order to maximize the number of hydrogen bonds that they can form with other species (19, 23). Thus, at the C₆₀ surface the two hydrogen atoms in the water molecule would orient toward the bulk solution and in turn present a positively charged interface. However, this is not the case for the *n*-C₆₀. A second somewhat related mechanism may explain the observed charge characteristics of the *n*-C₆₀.

This additional mechanism may be explained using a theory put forth by Andrievesky et al. (10) where the C₆₀ acquires charge through surface hydrolysis reactions. This was proposed by Andrievesky et al. (10), who stated that in the THF technique the C₆₀ first forms supramolecular complexes with THF, which then interact with water molecules and can be represented as {*m*C₆₀}:H₂O. On the other hand for the aqu/*n*-C₆₀, the C₆₀ molecule only interacts with water and in turn forms large clusters of hydrated C₆₀ and is thus represented as C₆₀:{H₂O}_{*n*} (10). In other words, charge transfer occurs between the alcoholic oxygen of the water molecule (electron donor) and the C₆₀ acting as the electron acceptor (4). The tendency of these bound water molecules to ionize (i.e., as they lose a hydrogen) with increasing pH results in the observed increase in the absolute value of the negative surface charge (Figure 3a). The presence of these large hydrated C₆₀ clusters is evidenced by the broad absorbance bands observed in the UV spectra for the aqu/*n*-C₆₀ (Figure 6). This interaction occurs for both the THF/*n*-C₆₀ and aqu/*n*-C₆₀, although the stronger charge imparted by the THF prevents the formation of the large hydrated clusters through electrostatic repulsion. Nevertheless, charge transfer from water appears to contribute to the overall *n*-C₆₀ surface charge in both cases.

In summary, fullerene clusters (*n*-C₆₀) are significantly charged in a spectrum of aqueous environments. The magnitude of this charge however is dependent on the

method used to prepare the $n\text{-C}_{60}$ due to the ability of C_{60} to acquire charge through a number of routes. Nevertheless, there appear to be two primary routes of charge acquisition for $n\text{-C}_{60}$, which both originate from the ability of the C_{60} to act as a strong electron acceptor: charge transfer and surface hydrolysis. The ability of C_{60} to acquire charge over time simply by mixing in water has significant implications for the transport of these materials in the environment. Contrary to expectations based on the native surface chemistry of the C_{60} molecule, these materials may become dispersed in water over time and become mobile as a result of their charge acquisition. However, on the basis of the results presented here, these materials are subject to classical electrostatic phenomena; therefore, their behavior in aqueous media may be manipulated according to established techniques.

Literature Cited

- (1) Kroto, H. W.; Heath, J. R.; O'Brien, S. C.; Curl, R. F.; Smalley, R. E. C_{60} -Buckminsterfullerene. *Nature* **1985**, *318*, 162–163.
- (2) Nakamura, E.; Isobe, H. Functionalized fullerenes in water. The first 10 years of their chemistry, biology, and nanoscience. *Acc. Chem. Res.* **2003**, *36*, 807–815.
- (3) Doome, R. J.; Fonseca, A.; Nagy, J. B. C-MAS-NMR investigation of solutions saturated with fullerenes: study of the anomalous solubility behaviour. *Colloids Surf. A* **1999**, *158*, 137–143.
- (4) Deguchi, S.; Rossitz, G. A.; Tsujii, K. Stable dispersions of fullerenes, C_{60} and C_{70} in water. Preparation and characterization. *Langmuir* **2001**, *17*, 6013–6017.
- (5) Avdeev, M. V.; Khokhryakov, A. A.; Tropin, T. V.; Andrievsky, G. V.; Klochkov, V. B.; Derevyanchenko, L. I.; Rosta, L.; Garamus, V. M.; Priezhev, V. B.; Korobov, M. V.; Aksenov, V. L. Structural features of molecular-colloidal solutions of C_{60} fullerenes in water by small-angle neutron scattering. *Langmuir* **2004**, *20*, 4363–4368.
- (6) Alargova, R. G.; Deguchi, S.; Tsujii, K. Stable colloidal dispersions of fullerenes in polar organic solvents. *J. Am. Chem. Soc.* **2001**, *123*, 10460–10467.
- (7) Adamenko, I. I.; Bulavin, L. A.; Moroz, K. O.; Prylutsky, Y. I.; Scharff, P. Equation of state for C_{60} toluene solution. *J. Mol. Liq.* **2003**, *105*, 149–155.
- (8) Andrievsky, G. V.; Klochkov, V. K.; Karyakina, E. L.; Mchedlov-Petrosyan, N. O. Studies of aqueous colloidal solutions of fullerene C_{60} by electron microscopy. *Chem. Phys. Lett.* **1999**, *300*, 392–396.
- (9) Andrievsky, G. V.; Klochkov, V. K.; Karyankina, E. L.; Mchedlov-Petrosyan, N. O. Studies of aqueous colloidal solutions of fullerene C_{60} by electron microscopy. *Chem. Phys. Lett.* **1999**, *300*, 392–396.
- (10) Andrievsky, G. V.; Klochkov, V. K.; Bordyuh, A. B.; Dovbeshko, G. I. Comparative analysis of two aqueous-colloidal solutions of C_{60} fullerene with help of FTIR reflectance and UV–vis spectroscopy. *Chem. Phys. Lett.* **2002**, *364*, 8–17.
- (11) Arbogast, J. W.; Darmany, A. P.; Foote, C. S.; Rubin, Y.; Diederich, F. N.; Alvarez, M. M.; Anz, S. J.; Whetten, R. L. Photophysical properties of C_{60} . *J. Phys. Chem.* **1991**, *95*, 11–12.
- (12) Guldi, D. M.; Prato, M. Excited-state properties of C_{60} fullerene derivatives. *Acc. Chem. Res.* **2000**, *33*, 695–703.
- (13) Mchedlov-Petrosyan, N. O.; Klochkov, V. K.; Andrievsky, G. V. Colloidal dispersions of fullerene C_{60} in water: some properties and regularities of coagulation by electrolytes. *J. Chem. Soc. Faraday Trans. I* **1997**, *93*, 4343–4346.
- (14) Kroto, H. W.; Allaf, A. W.; Balm, S. P. C_{60} : Buckminsterfullerene. *Chem. Rev.* **1991**, *91*, 1213–1235.
- (15) Da Ros, T.; Prato, M. Medicinal chemistry with fullerenes and fullerene derivatives. *Chem. Commun.* **1999**, 663–669.
- (16) Walther, J. H.; Jaffe, P. R.; Kotsalis, E. M.; Werder, T.; Halicioglu, T.; Koumoutsakos, P. Hydrophobic hydration of C_{60} and carbon nanotubes in water. *Carbon* **2004**, *42*, 1185–1194.
- (17) Hunter, R. J. *Foundations of Colloid Science*, Vol. I; Oxford University Press: New York, 1986.
- (18) Kadish, K. M.; Ruoff, R. S. *Fullerenes Chemistry, Physics, and Technology*; John Wiley & Sons: New York, 2000.
- (19) van Oss, C. J. *Interfacial Forces in Aqueous Media*; Marcel Dekker: New York, 1994.
- (20) Cheng, X.; Kan, A. T.; Tomson, M. B. Naphthalene adsorption and desorption from aqueous C_{60} fullerene. *J. Chem. Eng. Data* **2004**, *49*, 675–683.
- (21) Elimelech, M.; Gregory, J.; Jia, X.; Williams, R. A. *Particle Deposition and Aggregation: Measurement, Modelling, and Simulation*; Butterworth-Heinemann: Oxford, 1995.
- (22) Hunter, R. J. *Zeta Potential in Colloid Science: Principles and Applications*; Academic Press: London, 1981.
- (23) Israelachvili, J. N. *Intermolecular and Surface Forces*, 2nd ed.; Academic Press Harcourt Brace Jovanovich: London, 1992.
- (24) Stumm, W. *Chemistry of the Solid–Water Interface*; Wiley: New York, 1992.
- (25) Elimelech, M.; O'Melia, C. R. Effect of electrolyte type on the electrophoretic mobility of polystyrene latex colloids. *Colloids Surf.* **1990**, *44*, 165–178.
- (26) Childress, A. E.; Elimelech, M. Effect of solution chemistry on the surface charge of polymeric reverse osmosis and nanofiltration membranes. *J. Membr. Sci.* **1996**, *119*, 253–268.
- (27) Hunter, R. J. *Foundations of Colloid Science*; Clarendon Press: Oxford, 1989; Vol. 2.
- (28) Ravindran, S.; Wu, J. Overcharging of nanoparticles in electrolyte solutions. *Langmuir* **2004**, *20*, 7333–7338.
- (29) Moraru, V.; Lebovka, N.; Shevchenko, D. Structural transitions in aqueous suspensions of natural graphite. *Colloids Surf. A* **2004**, *242*, 181–187.
- (30) Stumm, W.; Morgan, J. J. *Aquatic Chemistry*, 2nd ed.; John Wiley & Sons: New York, 1981.
- (31) van Den Hul, H. J.; Vanderhoff, J. W. The characterization of latex particle surfaces by ion exchange and conductometric titration. *Electroanal. Chem. Interfacial Electrochem.* **1972**, *37*, 161–181.
- (32) Hunter, R. J. *Zeta Potential in Colloid Science*; Academic Press: New York, 1981.
- (33) Sayes, C. M.; Fortner, J. D.; Guo, W.; Lyon, D.; Boyd, A. M.; Ausman, K. C.; Tao, Y. J.; Sitharaman, B.; Wilson, L. J.; Hughes, J. B.; West, J. L.; Colvin, V. L. The differential cytotoxicity of water-soluble fullerenes. *Nano Lett.* **2004**, *4*, 1881–1887.
- (34) Nagy, G. Water structure at the graphite(0001) surface by STM measurements. *J. Electroanal. Chem.* **1996**, *409*, 19–23.

Received for review January 14, 2005. Revised manuscript received April 26, 2005. Accepted April 28, 2005.

ES050090D